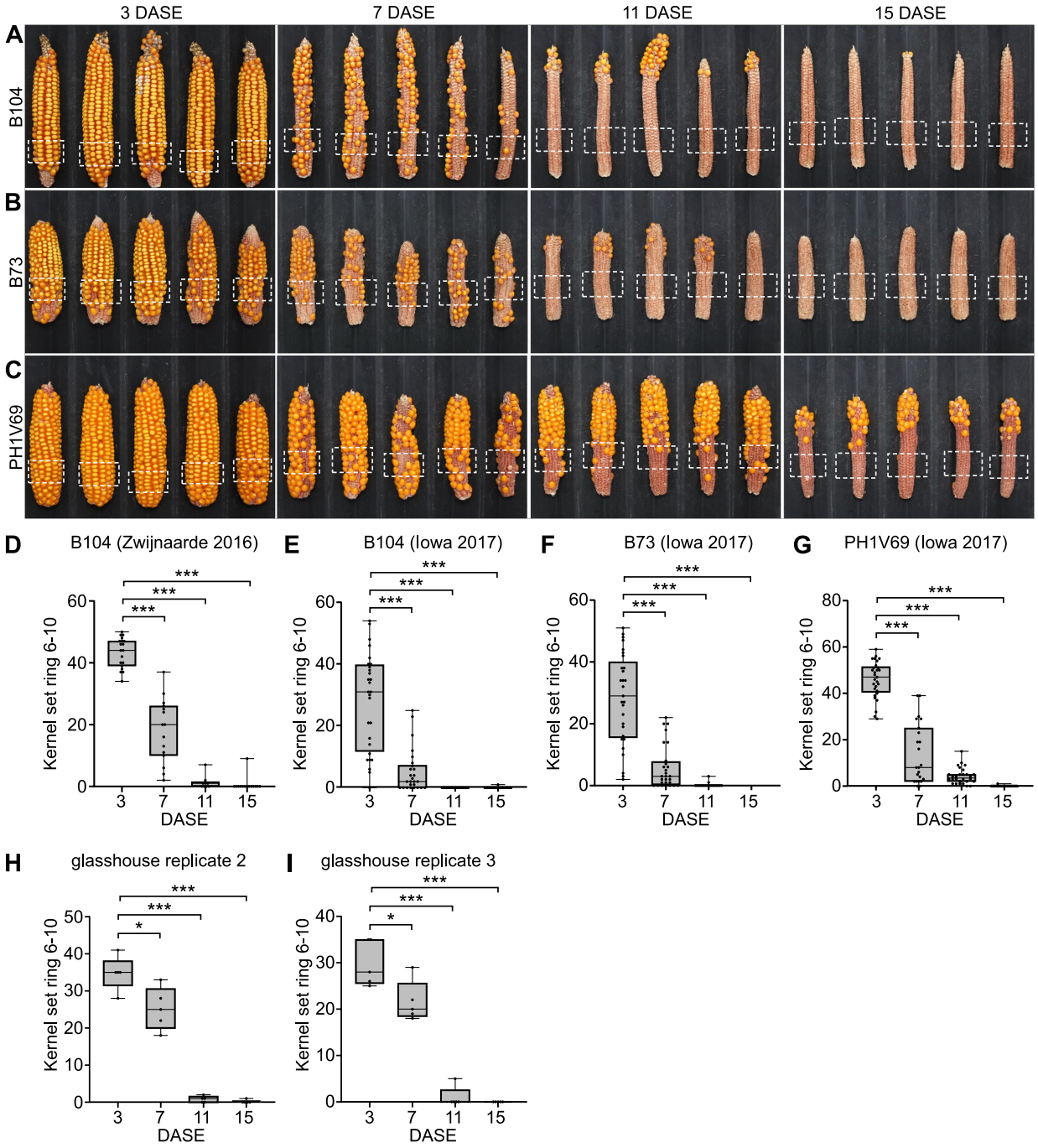

Supplemental Figure S1. Kernel set at rings 6-10 after manual synchronous pollination in field conditions.

Manual synchronous pollinations were performed at 3, 7 and 11 DASE, respectively and kernel set was evaluated in mid-base region of the ear (dashed rectangle). **(A-C)** Kernel set in the inbred lines B104, B73 and Ph1V69 is reduced upon synchronous pollination at late time points in field conditions. **(D)** In the field in Zwijnaarde (2016), the following values were recorded as a one-sided count at rings 6-10: 43.4 ± 4.85 (SD, n=19) at 3 DASE, 18.1 ± 10.3 (n=15) at 7 DASE, 1.3 ± 2.2 (n=9) at 11 DASE and only 0.6 ± 2.4 (n=14) at 15 DASE. **(E-G)**: Inbreds B73, B104 and PH1V69 were tested in the field in Iowa (2017). At 3 DASE one-sided kernel set recorded at ear rings 6-10 corresponded to an average of 28.2 kernels ± 14.55 (n=29) for B73; 28.0 kernels ± 15.6 (n=28) for B104 and 45.9 kernels ± 7.9 (n=29) for PH1V69 per side. At 7 DASE there was an average of 5.8 ± 5.2 (n=28) in inbred B73; 5.2 kernels ± 7.0 (n=26) in inbred B104 and 19.9

kernels ± 12.9 (n=23) in inbred PH1V69 per side. At 11 DASE there was an average of 0.2 ± 0.7 (n=19) for B73; no kernels (n=28) for inbred B104 and 4.3 kernels ± 3.4 (n=28) for PH1V69 per side. At 15 DASE the following values were recorded: 0.00 (SD=0.00, n=20) for B73; 0.06 kernels (SD=0.25, n=15) for B104 and 0.03 kernels (SD=0.17, n=33) for PH1V69 per side. **(H, I)** Quantification of kernel set in the mid-base region under glasshouse conditions for the second and third replicates of the data shown in Figure 1. Data are median values plotted with interquartile intervals. I: Average one-sided kernel set was 34.8 ± 4.6 (n=5) at 3 DASE, 25.2 ± 5.7 (n=5) at 7 DASE, 0.8 ± 0. 4 (n=5) at 11 DASE and 0.44 ± 0,20 (n=5) at 15 DASE for the second replicate. J: Similar values were obtained in the third replciate: kernel set was 29.8 ± 4.9 (n=5) at 3 DASE, 21.6 ± 4.4 (n=5) at 7 DASE, 1.0 ± 2.4 (n=5) at 11 DASE and 0.00 (SD=0,00, n=5) at 15 DASE. Statistical significances were calculated using student's t-test (*P<0.05; **P<0.01; ***P<0.001).

Supporting Figure 1.

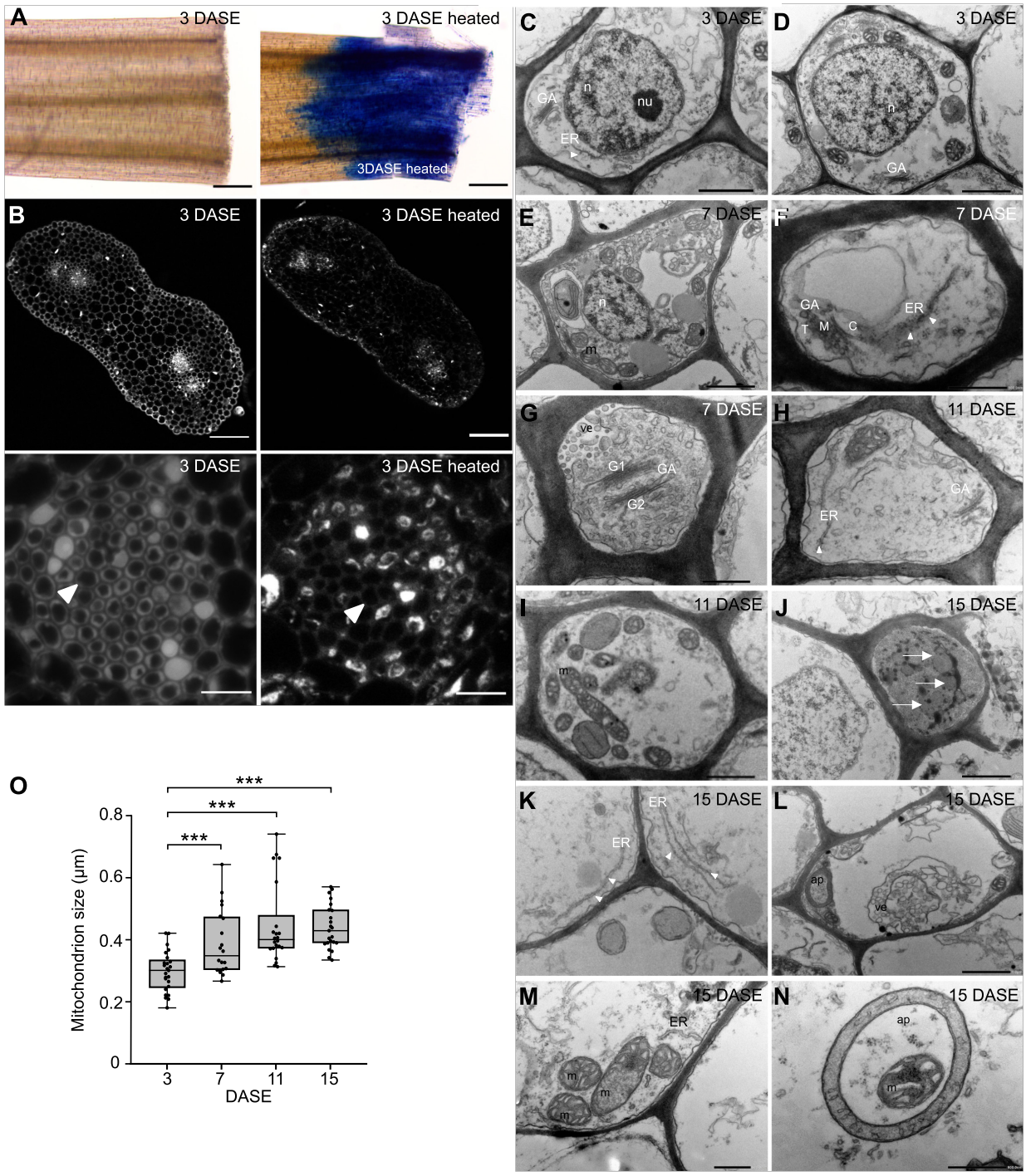

Supplemental Figure S2. The base of unpollinated senescent silk shows subcellular hallmarks of PCD.

(A) At 3 DASE no Evans Blue signal is detected in contrast to the heat-treated control.

(B) In the heat-treated 3 DASE sample, the parenchyma cells are damaged and torn, as visualized by autofluorescence of fixed cross sections of silk strands. Insets show details of TT at higher magnification; TT cells at 3 DASE have a regular morphology cytoplasm and vacuoles, while in the heat-treated sample, cells show cellular remains and more cells without a visible cytoplasm.

(C-D): TEM at 3 DASE; rough ER immediately adjacent to the cell nucleus (n) with many ribosomes (white arrowheads) attached to its cytoplasmic surface. At 3 DASE there is a large decondensed nucleus and small ER with small mitochondria of high electron density are present in the TT cells.
(E) At 7 DASE, irregularly shaped nuclei with condensed electron-dense chromatin and mitochondrial dimerization can be observed.
(F) Prominent amount of rough ER and enlarged GA at 7 DASE. 7 DASE: compartmentalization of the Golgi stack from the cis-face (C) close to ER, to medial cisternae (M) to the trans face (T) where the secretory vesicles form at their periphery.
(G) GA consisting of two Golgi stacks (G1, G2) and numerous vesicle (ve) in the cytoplasm (larger ones are product of trans Golgi.
(H) At 11 DASE, the Golgi complex undergoes disassembly. The interconnected ribbon structures of the Golgi complex are lost and Golgi-associated membranes are dispersing; ribosomes are detached from the swollen ER.
(I): Mitochondrial elongation at 11 DASE.
(J) nuclear disintegration at 15 DASE with apoptotic like nuclear bodies (black arrows).
(K) At 15 DASE, the ER appeared fragmented and devoid of ribosomes.
(L) At 15 DASE, multiple vesicles remain as well as ER-associated autophagosomes (ap).
(M) Swollen mitochondria with distortion and lysis of cristae at 15DASE.
(N) mitochondria enveloped in vesicular structures indicative of autophagic activities.
(O) Mitochondria increase in size during silk senescence. The mitochondrial diameter was quantified in the TEM section planes in transmitting tract. The average size of mitochondria measured was 0.29 µm ± 0.01 (SE, n=25) at 3 DASE 0.39 µm ± 0.02 (n=20) at 7 DASE, 0.45 ± 0.02 (n=22) at 11 DASE and 0.44 ± 0.01 (n=23) at 15 DASE. Student's t-test (*P<0.05; **P<0.01; ***P<0.001). Scale bars are 200 µm in (A), 100 µm in upper panel of (B), 10 µm in the lower panel of (B); 1 µm in (C-M), 500 nm in (N). *Black arrow, apoptotic-like body **ER,** endoplasmic reticulum; **GA,** Golgi apparatus; **TT**, transmitting tract**; n**, nucleus; **nc**, nucleolus; **m**, mitochondria, **ab**, apoptotic-like body; **ap**, autophagosome; **ve**, vesicles white arrowhead – ribosome.*
Supporting Figure 1.

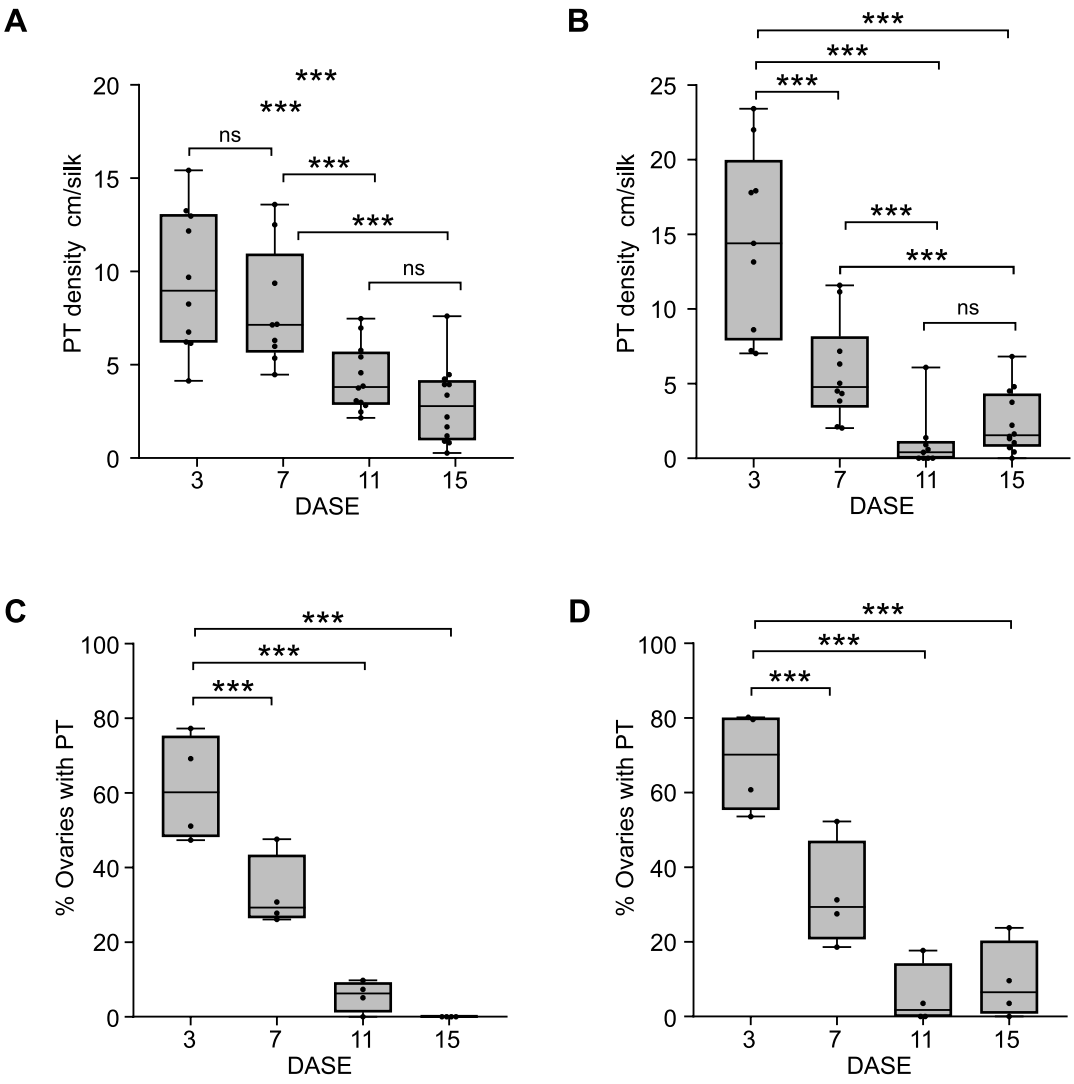

Supplemental Figure S3. PT density gradually decreases during silk senescence.

(A-B) PT density (number of pollen tubes per cm silk) sequentially decreases during silk senescence. A: Second replicate: PT density at 3 DASE is 9.5 ± 1.2 (SE, n=10); 8.0 ± 1.1 (n=10) at 7 DASE; 4.3 ± 0.5 (n=12) at 11 DASE; and 2.1 ± 0.6 (n=12) at 15 DASE. B: Third replicate: density at 3 DASE is 14.6 ± 2.1 (n=10); 5.8 ± 1.2 (n=10) at 7 DASE; 1.04 ± 0.61 (n=10) at 11 DASE; and 2.4 ± 0.60 (n=12) at 15 DASE.

(C) At 3 DASE on average 61.3% ± 7.2 (SE, n=226) of ovaries show GUS staining indicative of PT presence; at 7 DASE this percentage decreases to 33.1% ± 6.2 (n=212); to 5.6% ± 2.1 n(=205) at 11 DASE and to 0.0% (SD=0.0, n=200) at 15 DASE.

(D) The third replicate of the experiment shows that at 3 DASE on average 68.6% ± 6.7 (SE, n=216) of ovaries show GUS staining indicative of PT presence; at 7 DASE this percentage is reduced to 32.4% ± 7.1 (n=202); to 5.3% ± 4.2 (n=211) at 11 DASE; and to 9.2% ± 5.25 (SD, n=210) at 15 DASE. Student's t-test (***P<0.001; ns- non- significant) Approximately 40-55 ovaries were extracted from the mid-base region of 5 ears.

Supporting Figure 2F.

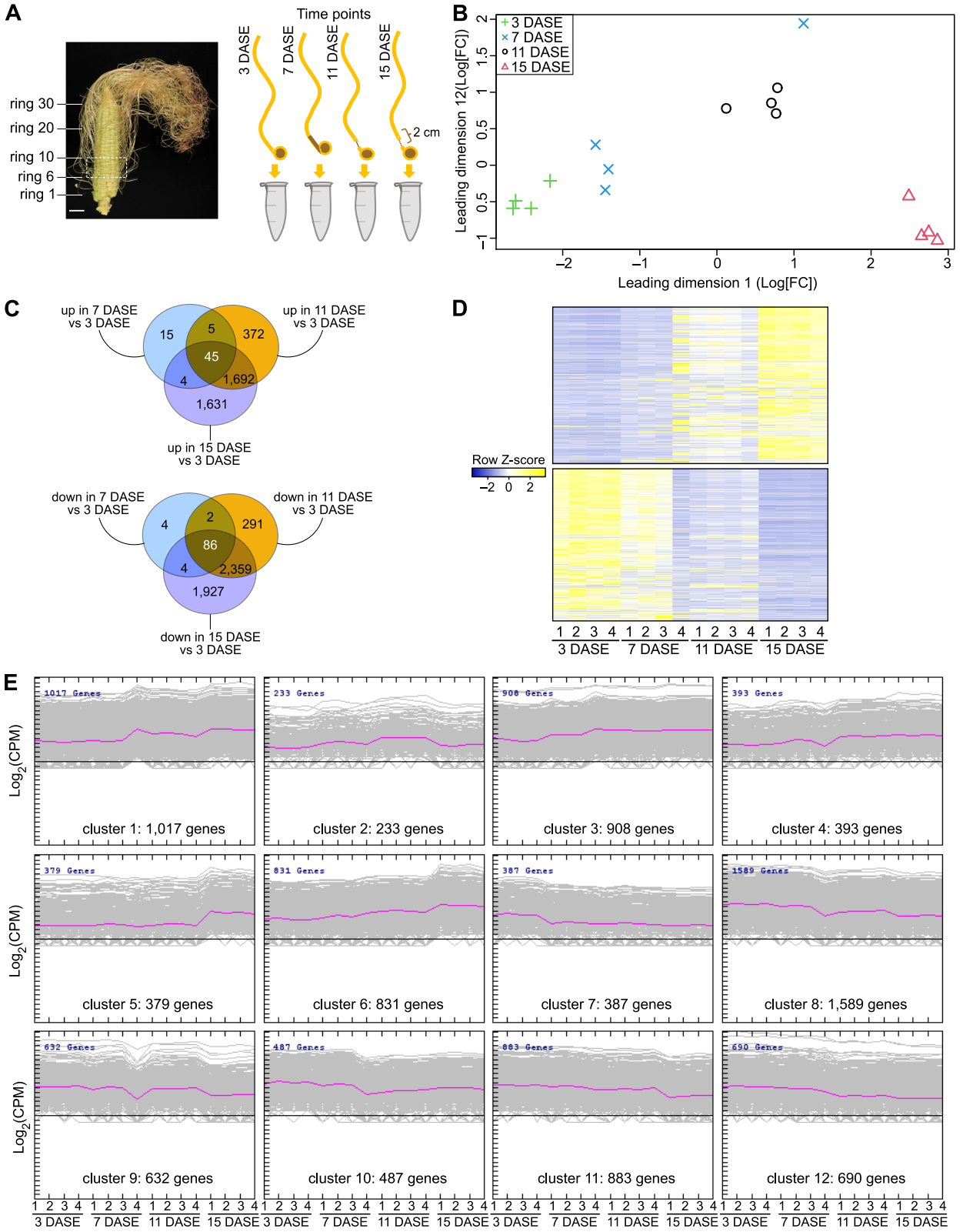

Supplemental Figure S4. Transcriptome analysis reveals differentially regulated genes during silk senescence.

(A) Schematic diagram describing the experimental set up of tissue sampling for RNA-seq. Only the silks belonging to rows 6 to 10 from the ear base were harvested and the two most basal cm were taken for RNA extraction. The sampling was done for four different time points over silk senescence (3, 7, 11, 15 DASE).
(B) MDS plot based on the 500 genes with highest fold-change in pairwise comparison.
(C) Venn diagrams showing the extent of overlap between the upregulated (up) and downregulated (bottom) DEGs during silk senescence.
(D) Heatmap representing the normalized expression value in the different RNA-seq samples of the genes with both a FDR<0.05 and a $Log_2FC>2$ (up) or $Log_2FC<-2$ (bottom) in at least one of the comparisons over time. **(E)** K-mean clustering of the DEGs over silk senescence. For each cluster, the Log_2-normalized expression of every gene is indicated for the different time points and for each replicate. The solid red lines indicate the mean expression trend for each cluster. Scale bar is 2 cm in (A).
Supporting Figure 4.

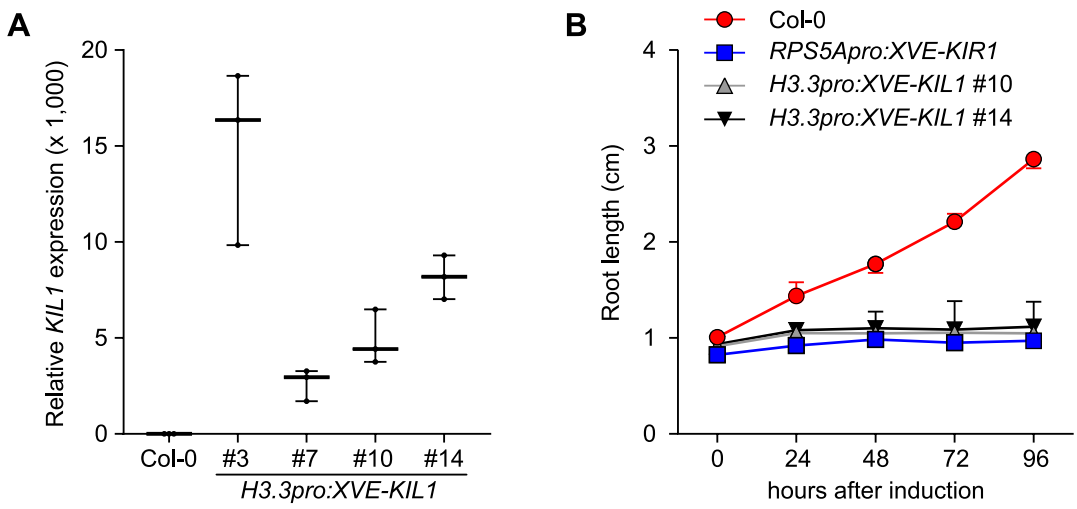

Supplemental Figure S5. KIL1 induces cell death in Arabidopsis.
(A) *KIL1* expression in the four independent *KIL1* overexpressing lines. The box and whisker plots display median values of three biological replicates with interquartile interval. (n=10, 5-day-old seedlings per replicate); expression values are relative to the reference gene *PEX4* (Gao et al., 2018).
(B) Estradiol induction of *KIL1* and *KIR1* overexpressing lines triggers root growth arrest in 5-day-old Arabidopsis seedlings. Graph represents median and standard error with interquartile range of three independent experiments; (n=10-15 seedlings per time point).
Supporting Figure 3E.

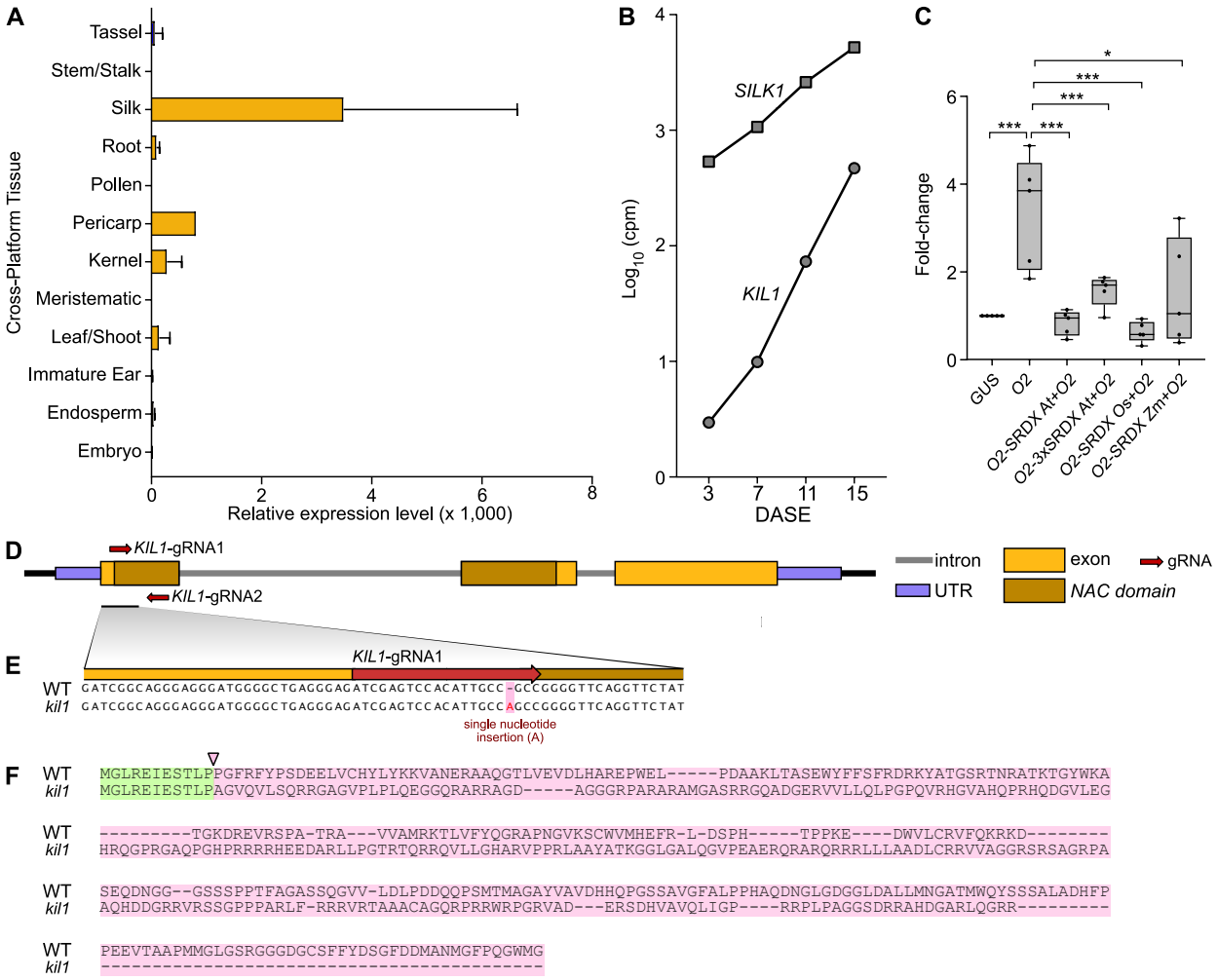

Supplemental Figure S6. Expression of *SILK*.

(A) *SILK1* is most highly expressed in silk tissue, however low expression can be detected in pericarp, ear leaf and husk leaves. The database represents a set of B73 expression profiling experiments covering different tissues and developmental timelines. Data processed using RSEM (RNA-seq by Expectation Maximization).
(B) RNA-seq from maize silk shows that *SILK1* is expressed at 3 DASE and its expression gradually increases during senescence similarly to the expression pattern of *KIL1*, albeit at a much higher level, making its promoter suitable as an overexpression tool.
(C) Transient expression assay testing the repression efficiency of various SRDX-type domains in maize leaf mesophyll protoplasts. We tested the repression efficiency of different SDRX motifs: 1) A modified SRDX domain from Arabidopsis (AtSRDX, LDLDLELRLGFA30); 2) A triple repeat of the same sequence (3xAtSRDX); 3) the original SUPERMAN SRDX domain (SUPD, DLDLELRLGFA31); and the SRDX motif of the maize RAMOSA1 protein (ZmSRDX, LDLELSL32). As a control, we used the interaction of the bZIP transcription factor Opaque2 with its cognate *Zein* promoter sequence33. The SRDX domain derived from rice (Os SRDX) and Arabidopsis (At SRDX) showed stronger repression activity than ZmSRDX and 3x AtSRDX. The error bars represent the standard deviation of five independent experiments (SD; n=5, *=P<0.05).
(D) Genome editing of *KIL1*. Two sgRNAs were designed to target the region of the KIL1 locus encoding the N-terminal NAC domain within exon 1.
(E) *KIL1*-qRNA1 leads to a single nucleotide, adenine (A), insertion resulting in premature termination of translation **(F)**. Abbreviations are: cons., nucleotide consensus; wt, wild type.
Supporting Figure 4A.

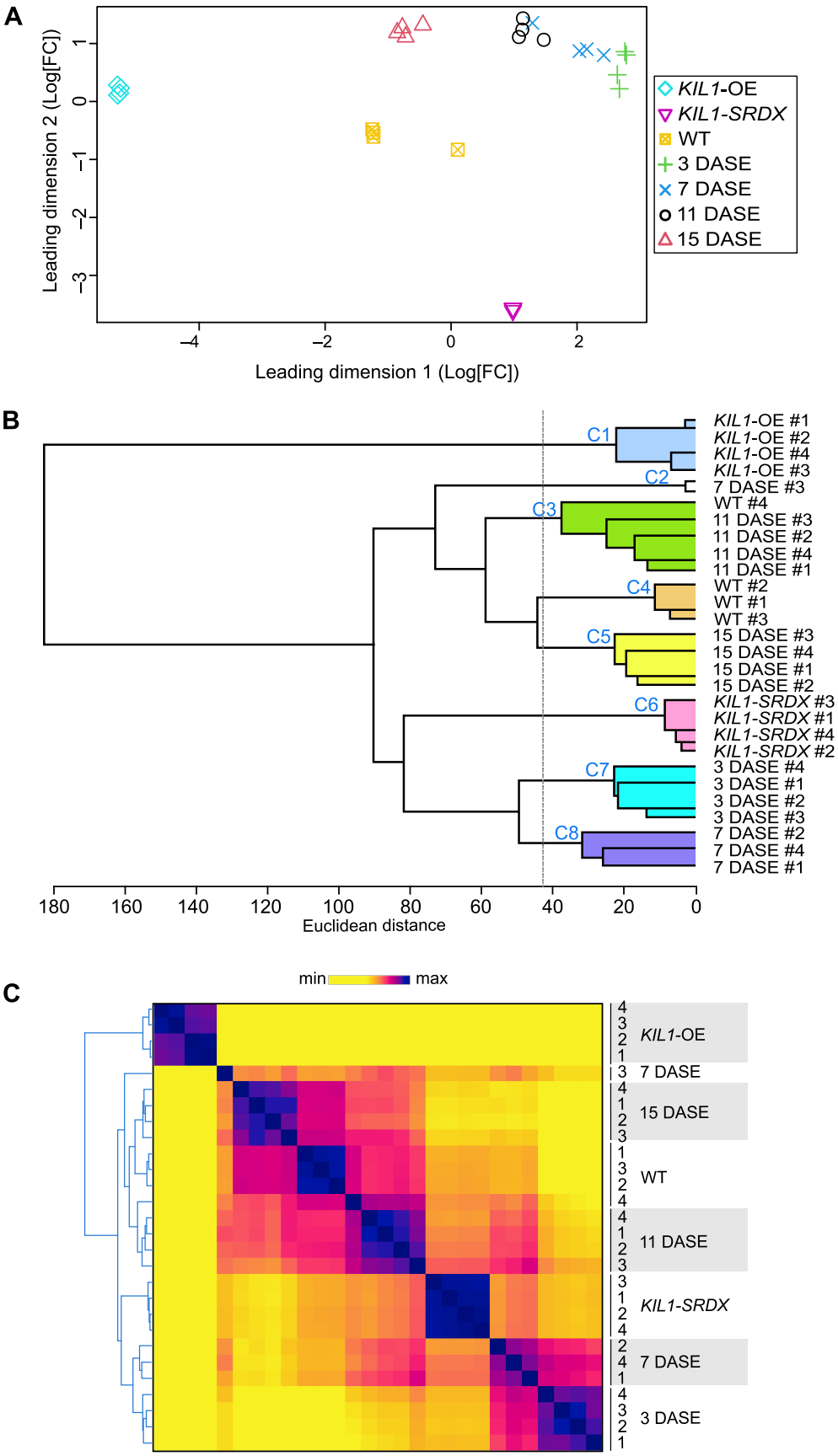
A
Leading dimension 2 (Log[FC])
Leading dimension 1 (Log[FC])
KIL1-OE
KIL1-SRDX
WT
3 DASE
7 DASE
11 DASE
15 DASE
B
C1
C2
C3
C4
C5
C6
C7
C8
KIL1-OE #1
KIL1-OE #2
KIL1-OE #4
KIL1-OE #3
7 DASE #3
WT #4
11 DASE #3
11 DASE #2
11 DASE #4
11 DASE #1
WT #2
WT #1
WT #3
15 DASE #3
15 DASE #4
15 DASE #1
15 DASE #2
KIL1-SRDX #3
KIL1-SRDX #1
KIL1-SRDX #4
KIL1-SRDX #2
3 DASE #4
3 DASE #1
3 DASE #2
3 DASE #3
7 DASE #2
7 DASE #4
7 DASE #1
Euclidean distance
C
min
max
KIL1-OE
7 DASE
15 DASE
WT
11 DASE
KIL1-SRDX
7 DASE
3 DASE

Supplemental Figure S7. *KIL1* depletion delays silk senescence.
(A) MDS plot based on the 500 genes with highest fold-change in pairwise comparison for the samples of both RNA-seq experiments performed at different silk senescence time points and RNA-seq comparing *KIL1*-OE, *KIL1-SRDX* line and WT at 11 DASE.
(B) Dendrogram resulting from a Hierarchical Clustering Analysis of all the samples, based on normalized Euclidean Distance. On the axis is indicated the average normalized Euclidean distance between the elements of two independent clusters.
(C) Distance heatmap resulting from a Hierarchical Clustering Analysis of all the samples, based on normalized Euclidean Distance. The color gradient from yellow to violet indicates an increase in the Euclidean Distance.
Supporting Figure 4.

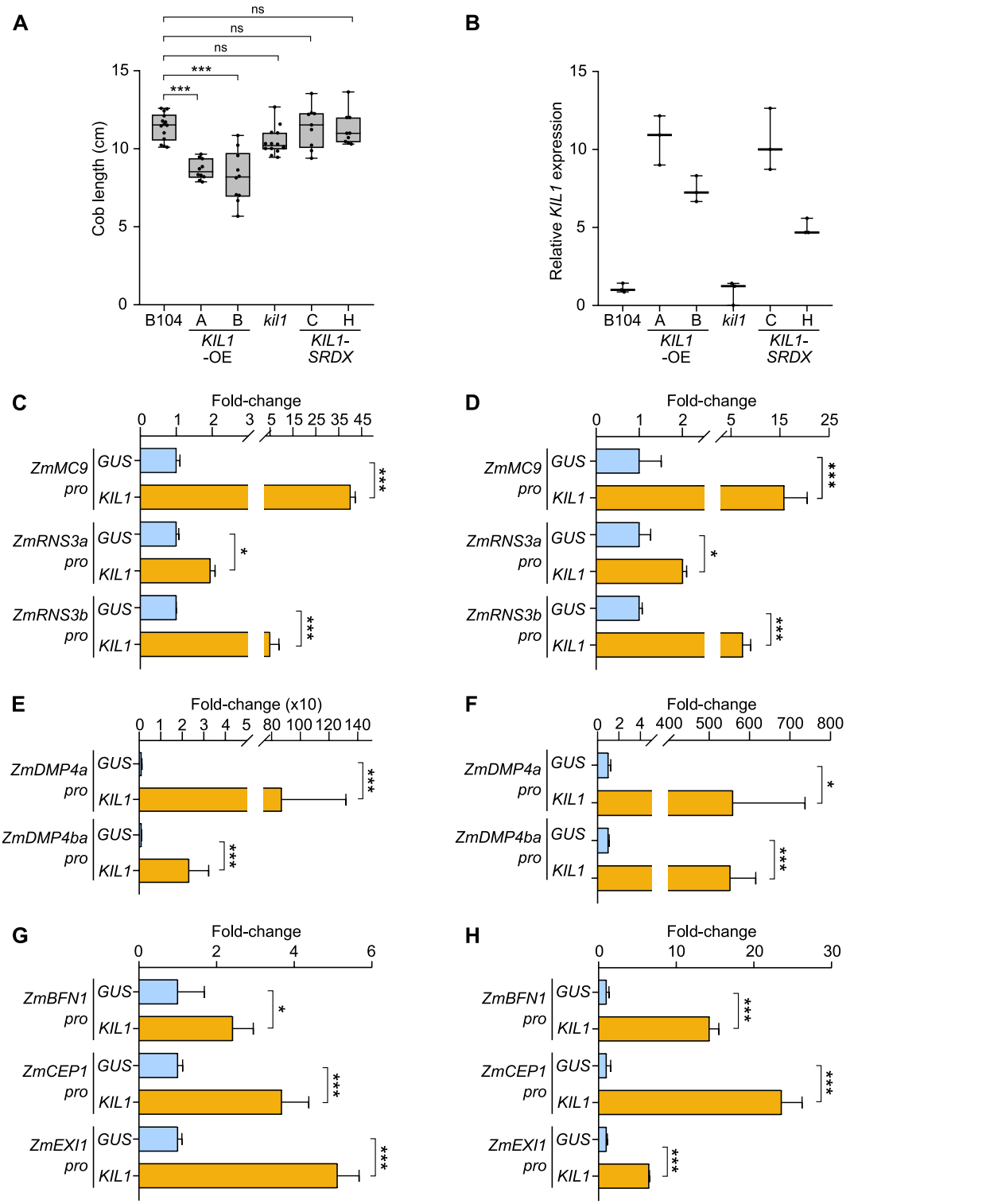

Supplemental Figure S8. *KIL1* overexpression reduces cob size and activates the expression of cell death-associated genes.

(A) *KIL1*-OE lines display small cobs. The average size of cob is 11.02 cm ± 0.23 (SE, n=14) in B104; significantly shorter in both *KIL1*-OE lines: 8.7cm ± 0.20 (n=10) and 8.2 cm ± 0.5 (n=10) in *KIL1*-OE A and *KIL1*-OE B, respectively. Cob length of loss of function lines is similar to wild type: 10.8 cm ± 0.2 (n=14) in

kil1; 11.4 cm ± 0.4 (n=10) in *KIL1-SRDX* C; 11.3 cm ± 0.4 (n=10) in *KIL1-SRDX* L. Student's t-test (**P*<0.05; ***P*<0.01; ****P*<0.001). Cobs of two independent experiments were measured.
(B) *KIL1* expression in the different transgenic lines. Mean values of three biological replicates are represented (n=20 silk bases per replicate); expression values are relative to the reference gene *ACTIN2*.
(C-H) *KIL1* is expressed in senescent silk and activates expression of putative maize cell-death associated genes. Promoter transactivation assay in maize leaf protoplasts for different putative dPCD promoters. The promoter activity was measured with a dual luciferase assay in presence of either *KIL1* or *GUS* gene. The activity measured was normalized by the mean value of the negative control (*GUS*) and the resulting fold-change is indicated in the graph. n=5, *=*P*<0.05; ***= *P*<0.001.
Supporting Figure 4.

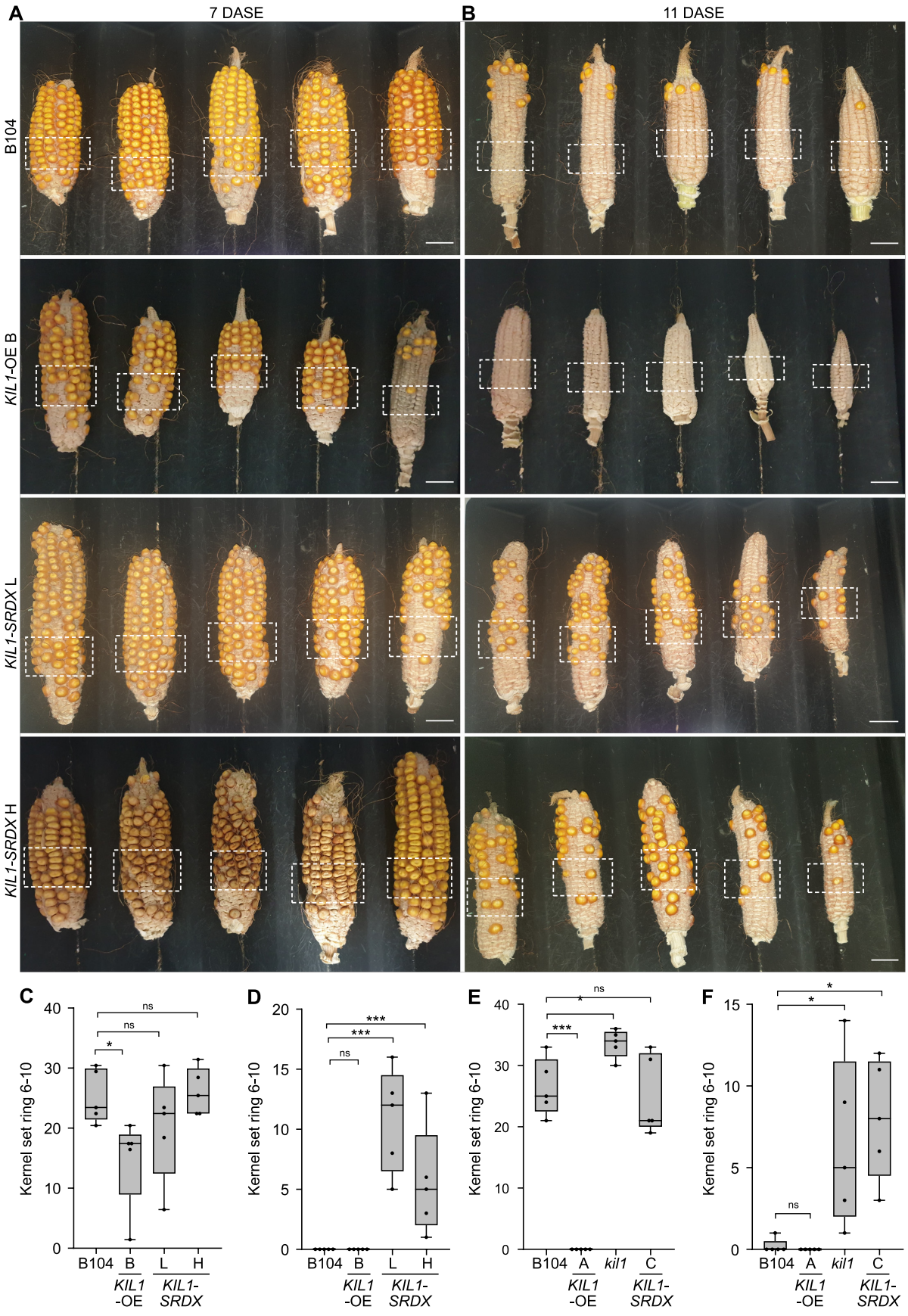
A
7 DASE
B
11 DASE
B104
KIL1-OE B
KIL1-SRDX L
KIL1-SRDX H
C
D
E
F
Kernel set ring 6-10
B104
B
L
H
A
kil1
C
KIL1 -OE
KIL1-SRDX
ns
*
***

Supplemental Figure S9. Overexpression of *KIL1* and loss of KIL1 function reduces or increases kernel set after late pollination of independent KIL transgenic lines, respectively.

(A-B) Manual synchronous pollination was performed at 7 and 11 DASE. **(A)** In comparison to the B104 wild-type, kernel set in the mid-base region of the ear (dashed rectangle) is drastically reduced in *KIL1*-OE B, while significantly increased in *kil1* and not changed in *KIL1-SRDX* H and *KIL1-SRDX* L at 7 DASE. **(B)** At 11 DASE kernel set in the mid-base region is drastically reduced in wt and KIL1_OE_B compared to 7DASE (A), while significantly increased in *kil1* and KIL1-SRDX_H and _L compared to wt at 11 DASE.

(C) Kernel set in the mid-base region under glasshouse conditions at 7 DASE. Data represent median values plotted with interquartile intervals. One-sided kernel set recorded was on average 25.0 ± 2.0 (SD, n=5) kernels in the wild type, 14.2 ± 3.4 (n=5) kernels in *KIL1*-OE B, 19.8 ± 14.0 (n=5) kernels in *KIL1-SRDX* L and 25.6 ± 1.75 (n=5) kernels in *KIL1-SRDX* H.

(D) Kernel set in the mid-base region at 11 DASE. Data represent median values plotted with interquartile intervals. One-sided kernel set recorded was on average 0.0 (SD=0.0, n=5) in the wild type, 0.0 (SD=0.0, n=5) in *KIL1*-OE B 1; 0.80 ± 1.9 (SD, n=5) in *KIL1-SRDX* L and 5.6 ± 2.0 (n=5) in *KIL1-SRDX* H**.**

(E) Second replicate of the pollination experiment from Figure 5. Kernel set in the mid-base region under glasshouse conditions at 7 DASE. Data represent median values plotted with interquartile intervals. One-sided kernel set recorded was on average 26.4 ± 2.1 (SD, n=5) kernels in the wild type; 0.0 (SD=0.0, n=5) kernels in *KIL*-OE A; 33.6 ± 1.0 (n=5) kernels in *kil1* and 25.0 ± 2.9 (n=5) kernels in *KIL1-SRDX* C.

(F) Second replicate of the pollination experiment from Figure 5. Kernel set in the mid-base region at 11 DASE. Data represent median values plotted with interquartile intervals. One-sided kernel set recorded was on average 0.20 ± 0.20 (SD, n=5) in the wild type; 0.0 (SD=0.0, n=5) in *KIL1*-OE A; 6.4 ± 2.3 (n=5) in *kil1*; and 8.0 ±3.7 (n=5) in *KIL1-SRDX* C. Scale bars are 2 cm.

Supporting Figure 5.

Supplemental Table S1. Number of reads and percentage mapped on the V3 version of the maize genome for each RNA-seq sample.

Sample name	Number of reads	% mapped
3 DASE #1	24,086,886	86.3
3 DASE #2	23,355,783	85.85
3 DASE #3	20,493,295	86.0
3 DASE #4	22,900,859	85.6
7 DASE #1	23,322,736	85.1
7 DASE #2	24,697,730	85.4
7 DASE #3	23,035,390	85.4
7 DASE #4	22,932,564	83.3
11 DASE #1	23,370,225	84.4
11 DASE #2	24,865,725	84.3
11 DASE #3	21,687,521	84.9
11 DASE #4	22,187,040	85.3
15 DASE #1	24,775,866	84.7
15 DASE #2	23,368,884	83.9
15 DASE #3	24,071,029	84.7
15 DASE #4	23,140,043	84.05

Supplemental Table S2. Top 10 most enriched GO terms for the DEGs at 15 DASE compared to 3 DASE.

Upregulated DEG at 15 DASE vs 3 DASE

GO term (biological process)	Number annotated genes in maize genome	Number annotated DEGs at 15 vs 3 DASE	Expected number	Fold-enrichment	Raw *p*-value	FDR
cell wall macromolecule catabolic process	34	10	2.21	4.53	2.56E-04	1.61E-02
defense response to bacterium	106	19	6.88	2.76	2.09E-04	1.34E-02
response to bacterium	118	21	7.66	2.74	1.09E-04	8.11E-03
carbohydrate transport	104	18	6.75	2.66	4.38E-04	2.40E-02
defense response to other organism	205	32	13.31	2.4	2.69E-05	2.30E-03
interspecies interaction between organisms	251	38	16.3	2.33	9.62E-06	1.10E-03
response to external biotic stimulus	226	34	14.68	2.32	3.61E-05	2.98E-03
response to other organism	226	34	14.68	2.32	3.61E-05	2.93E-03
response to biotic stimulus	259	38	16.82	2.26	1.52E-05	1.52E-03
defense response	425	55	27.6	1.99	7.78E-06	9.39E-04

Supplemental Table S2 (continued). Top 10 most enriched GO terms for the DEGs at 15 DASE compared to 3 DASE.

Downregulated DEG at 15 DASE vs 3 DASE

GO term (biological process)	Number annotated genes in maize genome	Number annotated DEGs at 15 vs 3 DASE	Expected number	Fold-enrichment	Raw *p*-value	FDR
auxin efflux	12	7	1.2	5.84	9.54E-04	2.89E-02
photosynthesis, light harvesting in photosystem I	31	17	3.1	5.49	5.07E-07	3.61E-05
auxin homeostasis	15	8	1.5	5.34	6.45E-04	2.09E-02
photosynthesis, light harvesting	36	19	3.59	5.29	1.72E-07	1.33E-05
establishment or maintenance of cell polarity	14	7	1.4	5.01	1.87E-03	4.86E-02
chlorophyll biosynthetic process	23	10	2.3	4.35	4.92E-04	1.71E-02
hormone transport	22	9	2.2	4.1	1.32E-03	3.87E-02
regulation of stomatal movement	27	11	2.7	4.08	4.04E-04	1.44E-02
cellular process involved in reproduction in multicellular organism	28	10	2.8	3.58	1.65E-03	4.62E-02
male gamete generation	28	10	2.8	3.58	1.65E-03	4.59E-02

Supplemental Table S3. Expression value and expression comparison for the different stages of silk senescence for a list of the closest orthologs of Arabidopsis dPCD genes that show an increase in expression during silk senescence.
Cluster number correspond to the K-mean clustering analysis displayed in Supplemental Figure S4E.

								3 vs 7 DASE		3 vs 11 DASE		3 vs 15 D
Gene ID V5	Gene ID V3	Name	cluster	mean 3 DASE	mean 7 DASE	mean 11 DASE	mean 15 DASE	Log_2FC	FDR	Log_2FC	FDR	Log_2FC
Zm00001eb039650	GRMZM2G456217	***ZmCEP1***	6	8.5	128.8	193.8	4151.3	3.86	0.065	4.43	0.003	8.88
Zm00001eb043930	GRMZM2G168744	***ZmBFN1***	5	95.5	57	65.3	311.3	-0.79	0.4078	-0.62	0.0407	1.66
Zm00001eb229790	GRMZM2G020146	***ZmSPL48***	6	302.3	354	615.8	2600.8	0.25	0.862	0.95	0.0059	3.06
Zm00001eb027840	GRMZM2G167584	***ZmEXI1***	6	10.5	29.5	38.3	177.5	1.55	0.3107	1.78	0.0015	4.04
Zm00001eb343640	GRMZM2G070013	***ZmDMP4b***	6	10	21.5	30.5	154.8	1.13	0.308	1.52	0.0048	3.91
Zm00001eb383510	GRMZM5G812126	***ZmDMP4a***	5	3	3.5	3	75.5	0.23	1	-0.05	1	4.57
Zm00001eb328300	GRMZM2G141322	***ZmRNS3b***	6	3	16.8	65.5	477.8	2.54	0.3875	4.33	0.0001	7.23
Zm00001eb041390	GRMZM2G161274	***ZmRNS3a***	5	38.8	41.8	42.5	430.8	0.12	0.9727	0.07	0.9503	3.44
Zm00001eb196150	GRMZM2G022799	***ZmMC9***	5	55.5	82.5	56.8	554.3	0.55	0.4503	-0.03	1	3.29

Supplemental Table S4. Number of reads and percentage mapped on the V3 version of the maize genome for each RNA-seq sample.

Sample name	Number of reads	% mapped
KIL1-OE #1	26,998,605	88.9
KIL1-OE #2	27,436,819	89.0
KIL1-OE #3	27,170,895	88.8
KIL1-OE #4	28,285,472	88.5
KIL1-SRDX #1	25,574,052	87.7
KIL1-SRDX #2	25,468,774	87.6
KIL1-SRDX #3	24,652,940	87.9
KIL1-SRDX #4	25,761,250	88.4
WT #1	30,085,610	86.6
WT #2	30,735,272	86.3
WT #3	26,293,204	86.8
WT #4	29,358,928	86.7

Supplemental Table S5. Gene ontology (GO) enrichment analysis.
Top 10 most strongly enriched GO terms ("biological process") during silk senescence (15 DASE vs 3 DASE), and the enrichment of the same GO terms in the DEGs in KIL1 OE and KIL1-SRDX lines. Values in bold indicate an FDR < 0.05.

Top 10 GO terms enriched in the DEGs *upregulated* at 15DASE vs 3DASE	**DEGs upregulated in *KIL1*-OE (fold change)**	**DEG downregulated in *KIL1-SRDX* (fold change)**
cell wall macromolecule catabolic process	**3.84**	**5.3**
defense response to bacterium	**2.67**	2.89
response to bacterium	**2.77**	2.75
carbohydrate transport	**2.62**	1.21
defense response to other organism	**2.18**	**2.37**
interspecies interaction between organisms	**2.04**	**2.23**
response to external biotic stimulus	**2.07**	2.15
response to other organism	**2.07**	2.15
response to biotic stimulus	**1.98**	2.09
defense response	**1.72**	1.78

Top 10 GO terms enriched in the DEGs *downregulated* at 15DASE vs 3DASE	**DEGs downregulated in *KIL1*-OE (fold change)**	**DEGs upregulated in *KIL1-SRDX* (fold change)**
auxin efflux	3.56	4.37
photosynthesis, light harvesting in photosystem I	**4.13**	**3.39**
auxin homeostasis	4.27	4.2
photosynthesis, light harvesting	**3.85**	**3.21**
establishment or maintenance of cell polarity	2.29	3.75
chlorophyll biosynthetic process	3.71	**4.11**
hormone transport	2.91	2.86
regulation of stomatal movement	2.77	2.72
cellular process involved in reproduction in multicellular organism	1.52	1.12
male gamete generation	1.52	1.12

Supplemental Table S6. Expression value and expression comparison between the WT and transgenic lines for the closest orthologs of Arabidopsis dPCD genes that show a significant increase in expression during silk senescence.

***KIL1*-OE vs WT**

Gene ID V4	Gene ID V3	Name	Log_2FC	FDR	mean WT	mean *KIL1 OE*
Zm00001d052433	GRMZM2G022799	***ZmMC9***	2.53	0.05860	1157,0	4630.0
Zm00001d032186	GRMZM2G161274	***ZmRNS3a***	2.79	0.00513	1183,5	5642.5
Zm00001d022228	GRMZM2G141322	***ZmRNS3b***	4.06	0.00077	1230,5	14071.5
Zm00001d046149	GRMZM5G812126	***ZmDMP4a***	4.38	0.00146	115,5	1655.3
Zm00001d009557	GRMZM2G070013	***ZmDMP4b***	1.79	0.06574	313,0	745.8
Zm00001d030529	GRMZM2G167584	***ZmEXI1***	3.26	0.00114	347,8	2288.5
Zm00001d014983	GRMZM2G020146	***ZmSPL48***	1.55	0.12625	5170,5	10372.0
Zm00001d032501	GRMZM2G168744	***ZmBFN1***	2.90	0.00615	432,0	2206.3
Zm00001d031971	GRMZM2G456217	***ZmCEP1***	3.53	0.02022	6237,8	49561.8

WT vs *KIL1-SRDX*

Gene ID V4	Gene ID V3	Name	Log_2FC	FDR	mean *KIL1-SRDX*	mean WT
Zm00001d052433	GRMZM2G022799	***ZmMC9***	6.39	0.00867	11.3	1157.0
Zm00001d032186	GRMZM2G161274	***ZmRNS3a***	5.59	0.00117	20.0	1183.5
Zm00001d022228	GRMZM2G141322	***ZmRNS3b***	5.47	0.00058	22.5	1230.5
Zm00001d046149	GRMZM5G812126	***ZmDMP4a***	7.28	0.00701	0.5	115.5
Zm00001d009557	GRMZM2G070013	***ZmDMP4b***	6.05	0.00410	3.8	313.0
Zm00001d030529	GRMZM2G167584	***ZmEXI1***	3.91	0.00146	18.8	347.8
Zm00001d014983	GRMZM2G020146	***ZmSPL48***	3.61	0.00832	345.5	5170.5
Zm00001d032501	GRMZM2G168744	***ZmBFN1***	4.69	0.00222	13.5	432.0
Zm00001d031971	GRMZM2G456217	***ZmCEP1***	7.29	0.00337	32.5	6237.8

Supplemental Table S7. Primers used in this study.

Name	Sequence (5' to 3')
TEA ttB1_pZmCEP1_F	GGGGACAAGTTTGTACAAAAAAGCAGGCTTTGAAACCGGTAAAATTGACATCATGCAG
TEAattB2_pZmCEP1_R	GGGGACCACTTTGTACAAGAAAGCTGGGTTCTCTGCTAGCTTCGCTCGCGCCGCTAG
TEA attB1_pDMP4a_F	GGGGACAAGTTTGTACAAAAAAGCAGGCTTTGATAGTCATATGGGATTAAATCACCATC
TEA attB2_pDMP4a_R	GGGGACCACTTTGTACAAGAAAGCTGGGTTCGTGGGGACGAATAACCAAGATGGATTG
TEA attB1_pDMP4b_F	GGGGACAAGTTTGTACAAAAAAGCAGGCTTTGCACGTCACACTTGGATTTCTACCTTC
TEA attB2_pDMP4b_R	GGGGACCACTTTGTACAAGAAAGCTGGGTTCGACCCGTCCGCACCAGATCGTCTTC
TEA attB1_ZmEXI1_F	GGGGACAAGTTTGTACAAAAAAGCAGGCTTTATACGCTTGACAATGGATGCAGTCGC
TEA attB2_ZmEXI1_R	GGGGACCACTTTGTACAAGAAAGCTGGGTTGGCCGATTGCTGGAGGACAAAACAGTC
gRNA2-KIL1	GGAAGGCCACCGGCAAGGACCGCG
gRNA1-KIL1	ACACATTGCCGCCGGGGTTCAGG
KIL1-gRNA1_F	TTTTGGTCTCAGGCAATCGAGTCCACATTGCCGCCGTTTTAGAGCTAGAAATAGC
KIL1-gRNA2_R	TTTTGGTCTCAAAACCCCATGGCTCTCGCGCGTGCTGCTTCTTGGTGCCGCG
KIL1_TIDE_F	CATCTAGCGCGTGTTTTGGGGTAG
KIL1_TIDE_R	TGCGCACAAGGAATATGAACATCTCG
KIL1-qPCR_R	CGCTGTCTTTCCGCTTCTG
KIL1- qPCR_F	CAAGTCCTGCTGGGTCATG
ACTIN2_F	TACCCGATTGAGCATGGCA-
ACTIN2_R	TCTTCAGGCGAAACACGGA